minimal. This established reference gravity station at Maitri can be used for any future gravity surveys in this part of Antarctica for geodynamic studies and also for monitoring temporal gravity changes by measurements at the same location from time to time. Temporal gravity changes can provide a constrain to the elastic rebound due to deglaciation, because any change in the ice mass will deform the earth, which will result in crustal displacement and gravity changes[4].

We have established two high precision reference absolute gravity stations, one in India at NGRI, and the other at Maitri, Antarctica using FG-5 AG meter. The absolute gravity values at these locations have a measurement accuracy of about ~ 2 μGal with an overall uncertainty of ~ 5 μGal. These examples of gravity measurements describe the expected range of gravity variations and the measurement precision of the instrument. A correlation between water level and gravity changes demonstrates the utility of absolute gravity measurements for hydrological studies. It also suggests that water-level information is necessary for removal of seasonal effects from long-term gravity data recorded for the study of temporal variation of gravity field. This effect would be negligible in places like Antarctica, where subsurface mass changes are little and thus the reported absolute gravity value can be used for temporal changes.

1. Niebauer, T. M., Sasegawa, G. S., Faller, J. E., Hilt, R. and Klopping, F., A new generation of absolute gravimeters. *Metrologia*, 1995, **32**, 159–180.
2. Zerbini, S., Richter, B., Negusini, M., Romagnioli, C., Simon, D., Domenichini, F. and Schwahn, W., Height and gravity variations by continuous GPS, gravity and environmental parameter observations in the southern Po Plain, near Bologna, Italy. *Earth Planet. Sci. Lett.*, 2001, **1922**, 67–297.
3. Lambert, A., Courtier, N., Sasagawa, G. S., Klopping, F., Winester, D., James, T. S. and Liord, J. O., New constraints on Laurentide postglacial rebound from absolute gravity measurements. *Geophys. Res. Lett.*, 2001, **28**, 2109–2112.
4. Wahr *et al.*, Using GPS and gravity to infer ice mass changes in Greenland. *EOS*, 81, 2000, **37**, 421; 426–427.
5. Williams, S. D. P., Baker, T. F. and Jeffries, G., Absolute gravity measurements at UK tide gauges. *Geophys. Res. Lett.*, 2001, **28**, 2317–2320.
6. Emery, K. O. and Aubrey, D. G., Tide gauges of India. *J. Coastal Res.*, 1989, **5**, 489–501.
7. Tiwari, V. M., Cabane, C., Do Minh, K. and Cazenave, A., Sea level in the Indian Ocean from Topex-Poseidon altimetry and tide gauge. In *Oceanology* (ed. Gupta, H. K.), Universities Press, Hyderabad, India, 2005.
8. Bendick, R. and Bilham, R., Search for buckling of the southwest Indian coast related to Himalayan collision. *Geol. Soc. Am., Spec. Pap.*, 1999, **328**, 313–321.
9. Peter, G., Moose, R. E. and Wessells, C. W., High precision absolute gravity observations in the United States. *J. Geophys. Res.*, 1989, **94**, 5659–5674.
10. Manual of FG-5 available at www.microgsolutions.com
11. Wenzel, H. G., The nano-gal software: data processing package ETERNA 3.3. *Bull. Inf. Marées Terrestres*, 1996, **124**, 9425–9439.
12. Van Camp, M., Vauterin, P., Wenzel, H-G., Schott, P. and Francis, O., Accurate transfer function determination for super conducting gravimeters. *Geophys. Res. Lett.*, 2000, **27**, 37–40.
13. Allis, R. G. and Hunt, T. M., Analysis of exploitation induced gravity changes at Wairaki Geothermal field. *Geophysics*, 1986, **51**, 1647–1660.

ACKNOWLEDGEMENTS. We are grateful to Dr H. K. Gupta, former Secretary, DOD, Govt of India, who inspired us to start Absolute Gravity measurements in India and Antarctica. We thank Dr V. P. Dimri, Director, NGRI for encouragement and support. We acknowledge financial support received from CSIR and DOD for the purchase of this equipment. We also thank Dr Shakeel Ahmed and Dr D. Muralidharan for providing water-level data. V.M.T. and M.B.S.V. thank the leader and logistic team members of the 23rd Indian Antarctic Scientific Expedition and Director Logistic, NCAOR, Goa for support during the expedition.

Received 20 May 2005; revised accepted 1 April 2006

Muzaffarabad earthquake of 8 October 2005 (*Mw* 7.6): A preliminary report on source characteristics and recorded ground motions

S. K. Singh[1,*], A. Iglesias[2], R. S. Dattatrayam[3], B. K. Bansal[4], S. S. Rai[5], X. Perez-Campos[1], G. Suresh[3], P. R. Baidya[3] and J. L. Gautam[3]

[1]Instituto de Geofisica, UNAM, CU, 04510 Mexico, D.F., Mexico
[2]Instituto de Ingenieria, UNAM, CU, 04510 Mexico, D.F., Mexico
[3]India Meteorological Department, Lodhi Road, New Delhi 110 003, India
[4]Department of Science and Technology, New Mehrauli Road, New Delhi 110 016, India
[5]National Geophysical Research Institute, Uppal Road, Hyderabad 500 007, India

We present a preliminary source study of the Muzaffarabad earthquake of 8 October 2005 (*Mw* 7.6) and the far-field ground motions that it generated. Our analysis is based on regional broadband seismograms recorded at stations operated by the India Meteorological Department (IMD) which are situated to the south of the epicentre, and at non-IMD stations which are located to the north. We find that the source spectrum of the earthquake is reasonably consistent with ω^2-source model with a seismic moment, M_0, of 2.94×10^{20} N-m and a corner frequency, fc, of 0.051 Hz (Brune stress drop of 9.5 MPa). The radiated seismic energy, E_R, estimated from the empirical Green's function (EGF) technique is 2.70×10^{16} J. This yields a normalized radiated energy, E_R/M_0, of 9.1×10^{-5}, and an apparent stress, τ_a, of 2.7 MPa. The rupture area of

*For correspondence. (e-mail: krishna@ollin.igeofcu.unam.mx)

100×15 km^2 (estimated from slip distribution mapped from the inversion of teleseismic body waves) gives a static stress drop of about 11.3 MPa. From these source parameters we estimate a radiation efficiency of 0.49, implying a 'brittle' rupture typical of interplate events. Stochastic method requires a stress drop of ~10 MPa to explain the observed peak ground motions (A_{max} and V_{max}) recorded at regional distances, and predicts A_{max} and V_{max} exceeding 1 g and 100 cm/s, respectively at hard sites in the epicentral region. The source parameters and far-field ground motions of the Muzaffarabad and Bhuj earthquakes are quite similar even though the tectonic environment and the depth of their occurrence are distinct.

Keywords: Ground motions, Muzaffarabad earthquake, source parameters, source spectrum.

THE Muzaffarabad earthquake of 8 October 2005 is the largest event to occur along the Himalayan arc in the last 54 years. Harvard centroid moment tensor (CMT) catalogue[1] reports a seismic moment, M_0, of 2.94×10^{20} N-m (Mw 7.6). The location and focal mechanism of the earthquake (Figure 1; Table 1) show that it was a thrust event that occurred at a shallow depth in the western end of the India–Eurasia plate interface. The deaths, injuries, and destruction caused by the earthquake are a reminder of the seismic hazard faced by population centres along the foothills of the Himalayas and the plains to the south. Clearly, it is important to study this earthquake in as much detail as possible, so that seismic hazard posed by future large/great earthquakes in the region may be realistically estimated and mitigated.

Apparently, the earthquake was not recorded in the near-source region by strong-motion stations. The nearest accelerograms available to us are from Jammu (JMU) and Thien (THN) stations, located at epicentral distances of 226 and 300 km respectively (Figure 1). For this reason, we must rely on field observations and geodetic data in the epicentral region, geodetic measurements using space techniques, and regional and teleseismic seismograms to study the source characteristics of the earthquake and the ground motions that it produced.

Slip distribution on the fault plane of the earthquake has been mapped from the inversion of teleseismic body waves in two studies[2,3]. The preferred fault plane in both these studies roughly coincides with one of the nodal planes of Harvard CMT solution (azimuth 333°, dip 39° and rake 121°). Although the detail of slip distribution differs, both studies show (a) bilateral rupture, (b) small slip near the hypocentre, and (c) the largest slip occurring up-dip, about 25 to 30 km NW of the hypocentre. A second region of relatively large slip is located 20 to 30 km SE of the hypocentre. The rupture reaches the surface in one of the inversions[2]. Large surface or near-surface slip of about 5 m is confirmed from satellite imaging techniques[4,5].

Here we analyse broadband seismograms recorded at stations operated by India Meteorological Department (IMD), to the south of the rupture area ($131° \le \phi \le 180°$ and $880 \le \Delta \le 2090$ km, where ϕ is the azimuth of the station and Δ is the epicentral distance) and by agencies in other countries to the north ($-20° \le \phi \le 12°$; $820 \le \Delta \le 2655$ km). Our goal is to study the source characteristics of the earthquake and far-field ground motions that it generated. We estimate ground motions in the near-source region using the stochastic method. The results, although preliminary, provide a seismological framework to understand the disaster caused by the Muzaffarabad earthquake. We also compare this event with the Bhuj earthquake of 26 January 2001 (Mw 7.6), which occurred in the 'stable' continental region, about 1250 km to the SSW (Figure 1). The comparison allows us to investigate whether the source parameters and ground motions of these two same 'size' earthquakes, occurring in two distinct tectonic environments in the Indian subcontinent, are significantly different. This information could also be gainfully used in the estimation of ground motions from future earthquakes in the region.

We estimated the source spectrum of the Muzaffarabad earthquake from Lg waves. The median source displacement, velocity, and acceleration spectra [$\dot{M}_0(f)$, $f\dot{M}_0(f)$,

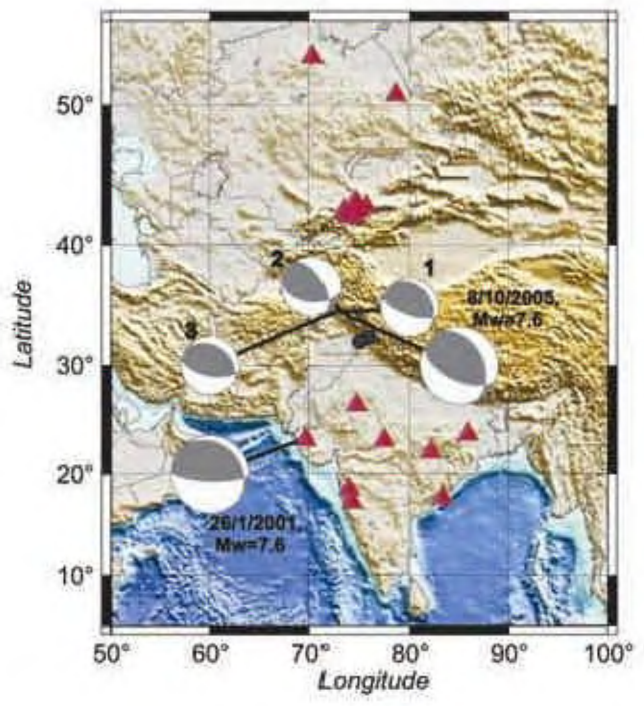

Figure 1. Map showing epicentres and focal mechanisms of the mainshock and three aftershocks of the Muzaffarabad earthquake used as empirical Green's functions in this study. Regional seismological stations whose recordings were used in this study are indicated by triangles. Two closest accelerographic stations which recorded the event are marked by solid dots. Also plotted are epicentre and focal mechanism of the 2001 Bhuj earthquake.

Table 1. Source parameters of the Muzaffarabad earthquake and its aftershocks used as empirical Green's functions

Date	Latitude °N	Longitude °E	Depth (km)	M_0 (N-m)	Mw	Focal mechanism		
						Strike	Dip	Rake
8 Oct. 2005; 03:50:52	34.37	73.47	12.0	2.94×10^{20}	7.6	333°	39°	121°
8 Oct. 2005; 12:08:32	34.56	73.11	15.5	4.55×10^{17}	5.7	326°	26°	124°
8 Oct. 2005;12:25:21	34.61	73.30	16.8	4.42×10^{17}	5.7	330°	57°	126°
19 Oct. 2005; 02:33:33	34.76	73.05	12.0	3.18×10^{17}	5.6	304°	32°	109°

Source parameters from Harvard CMT catalogue.

$f^2 \dot{M}_0(f)$, respectively] are shown in Figure 2 and are compared with the corresponding spectra of the Bhuj earthquake. [$\dot{M}_0(f)$ is also called the moment rate function, MRF.] The method of estimation of the spectra is described in a previous source study of the Bhuj earthquake[6]. Here we list some of the parameters used in the calculations of source spectra of both earthquakes; others were taken to be the same as those used in the Bhuj study[6]. Because of the shallow depth of the Muzaffarabad source[2–5], we took $\rho = 2.7$ g/cm^3 and $\beta = 3.35$ km/s, where ρ and β are density and shear-wave velocity in the source region. The corresponding values for the Bhuj earthquake were: $\rho = 2.85$ g/cm^3 and $\beta = 3.5$ km/s. The geometrical spreading, $G(R)$, was taken as $G(R) = R^{-1}$ for $R \le R_x$ and $G(R) = (RR_x)^{-1/2}$ for $R > R_x$, with $R_x = 100$ km. We note that the previous source analyses of the Bhuj earthquake[6,7] were based on $Q = 508f^{0.48}$, estimated from the recordings of the Jabalpur earthquake of 21 May 1997 (Mw 5.8)[8]. Here we have taken $Q = 800f^{0.42}$, since this estimate of Q for the Indian shield region is based on a larger dataset[9]. The paths from the Muzaffarabad earthquake to the IMD stations, however, are not entirely through the shield region. We estimated Q for these paths by requiring that the earthquake follow an ω^2-source model at high frequencies. This constrain was reasonably well fulfilled by choosing $Q = 500f^{0.62}$. The paths to non-IMD stations, which are located to the north of the source, include the region of active tectonics where Q is expected to be relatively low. We use $Q = 300f^{0.62}$ for this region since this functional form yields, roughly, an ω^2 spectrum. Figures 2 *a* and *b* illustrates the source spectra obtained from IMD and non-IMD data respectively.

An examination of the spectra in Figure 2 *a* suggests that they are reliable in the frequency range of 0.04 to 5.0 Hz. The spectra of Muzaffarabad earthquake are higher than those of the Bhuj earthquake for $0.04 \le f \le 0.5$ Hz. They also show a relative maximum at $f =$ 0.1 Hz and a minimum at 0.16 Hz. This maximum and minimum in the spectra can be explained by the interference of signals from the two patches of large slip on the fault plane mapped from inversion of teleseismic body waves[2,3]. The source spectra of the Muzaffarabad and Bhuj earthquakes are nearly identical at $f > 0.4$ Hz. Superimposed on the source displacement and acceleration spectra in Figure 2 *a* are the theoretical spectra from an ω^2-source model with $M_0 = 3.0 \times 10^{20}$ N-m and a corner frequency fc of 0.051 Hz. We note that the theoretical and observed spectra match reasonably well for both events.

The source spectra of the Muzaffarabad earthquake estimated from non-IMD data (Figure 2 *b*) differ somewhat from the corresponding spectra obtained from the IMD data (Figure 2 *a*). The spectra at the stations to the north have relatively smaller amplitudes. As shown in Figure 2 *b*, the observed spectra are explained well by the theoretical spectra from a ω^2-source model with $M_0 = 3.0 \times 10^{20}$ N-m and $fc = 0.051$ Hz.

Following Brune[10], stress drop ($\Delta\sigma_B$), M_0 and fc are related by: $fc = 0.49\beta(\Delta\sigma_B/M_0)^{1/3}$. This yields $\Delta\sigma_B = 9.5$ MPa and 10.8 MPa for the Muzaffarabad and Bhuj events respectively. We conclude that the Muzaffarabad and Bhuj earthquakes, which have the same M_w, also have similar source spectra.

An important source parameter of an earthquake is the radiated seismic energy, E_R. Based on teleseismic P-waves, G. Choy (written communication, 2006) and H. Kanamori (written communication, 2006) report $E_R = 0.29 \times 10^{16}$ and 1.1×10^{16} J respectively, for the Muzaffarabad event. For comparison, E_R of Bhuj earthquake, estimated using different methods[7,11], was ~2.1×10^{16} J. Relatively low E_R for the Muzaffarabad earthquake is not in agreement with the source spectra shown in Figure 2 *a* and *b* (middle frames), since E_R is given by the relation[12]:

$$E_R = (4\pi/5\rho\beta^5)\int_0^\infty f^2 \dot{M}_0^2(f)\,df, \qquad (1)$$

and $f\dot{M}_0(f)$ of the Muzaffarabad earthquake is roughly equal or even slightly greater than that of the Bhuj earthquake. We note, however, that there is a larger uncertainty in $f\dot{M}_0(f)$ of the Muzaffarabad earthquake, since the Q correction for paths to IMD and non-IMD stations is only approximate. A rough estimation of E_R can be obtained by assuming an ω^2-source model which is supported by Figure 2. For this model, eq. (1) reduces to $E_R = \pi^2 M_0^2 fc^3/5\rho\beta^5$. With $M_0 = 2.94 \times 10^{20}$ N-m, and $fc = 0.051$ Hz, we obtain $E_R = 2.0 \times 10^{16}$ J, roughly seven and two times larger than the values estimated by Choy and Kanamori respectively.

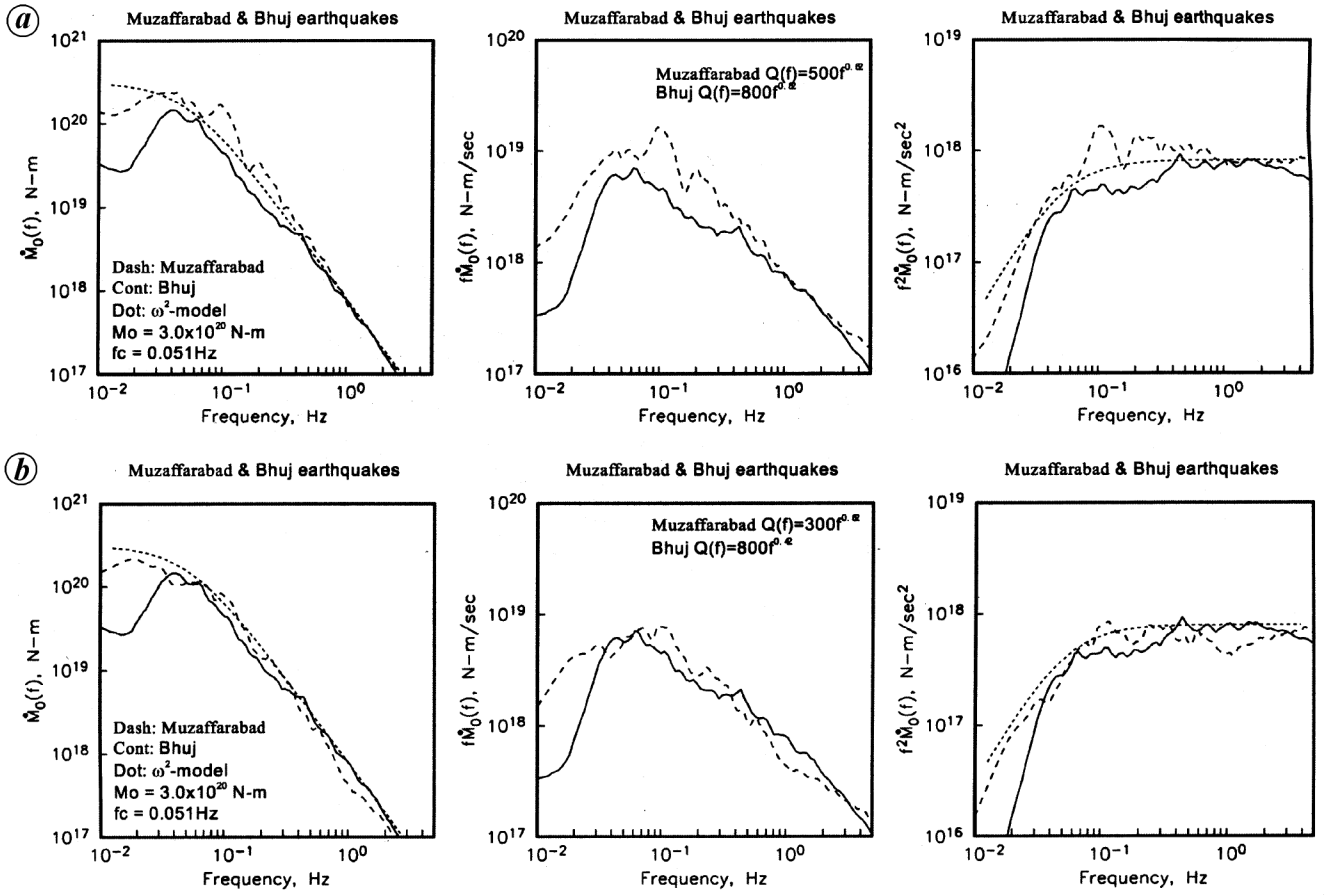

Figure 2. Median source spectra of Muzaffarabad and Bhuj earthquakes (dashed and continuous curves respectively) computed from Lg waves recorded at regional stations. (Left) Source displacement (or moment rate) spectrum, $\dot{M}_0(f)$. (Middle) Source velocity spectrum, $f\dot{M}_0(f)$. (Right) Source acceleration spectrum, $f^2\dot{M}_0(f)$. Dotted curves correspond to ω^{-2} source model with $M_0 = 3.0 \times 10^{20}$ N-m and corner frequency of 0.051 Hz. (*a*) Data from IMD stations all of which are located to the south of the source region. (*b*) Data from non-IMD stations.

To obtain a more reliable estimation of E_R, we used the empirical Green's function (EGF) technique[7,13]. This technique requires selection of aftershocks which have nearly the same location and focal mechanism as the mainshock. The aftershocks act as EGFs. The division of the mainshock spectrum by an aftershock spectrum recorded at the same station eliminates the path and site effects (two important sources of uncertainty in the estimation of E_R) and yields the shape of the source spectrum of the mainshock at frequencies smaller than the corner frequency of the aftershock. Multiplication of this spectrum by M_0 of the aftershock gives the moment rate spectrum, $\dot{M}_0(f)$. E_R is then computed using eq. (1). Table 1 lists three aftershocks which were deemed suitable as EGFs. Vertical component of the records were used in the study.

Figures 3 *a* and *b* illustrates the MRFs retrieved by the EGF technique (left frames). Frames on the right show median MRF obtained from (i) the EGF technique (continuous curves), (ii) directly from the spectra of mainshock recordings (long dashed curves, see also Figure 2), and (iii) the ω^2 model (short dashed curves, see also Figure 2). We required that at very low frequencies the MRFs obtained from the EGF technique using IMD data match the MRF from the ω^2-source model. To accomplish this, we had to decrease, M_0 of the first aftershock in Table 1 by 12% and increase the M_0 of the third aftershock by 57%. No change in the M_0 of the third aftershock was required. We note that the MRFs from the EGF technique deviate from the ω^2 model above 0.2 Hz. For this reason, we computed E_R by integrating eq. (1) from 0.01 to 0.15 Hz. The radiated energy for $f > 0.15$ Hz was estimated from the ω^2-source model as 8.6×10^{15} J. Figure 4 shows E_R as a function of azimuth. The median E_R is 2.70×10^{16} J. This value is nearly an order of magnitude greater than that obtained by Choy and 2.5 times the value given by Kanamori. Generally, recent estimates of E_R of the same earthquake by different authors differ by a factor of 2 to 3. Thus, the values of E_R reported by Kanamori and in this study are within the usual range of uncertainty. On the other hand, E_R reported by Choy seems too low. In further calculations, we take $E_R = 2.70 \times 10^{16}$ J. The normalized radiated seismic energy, E_R/M_0, is 9.14×10^{-5}. The apparent stress, τ_a, defined by $\tau_a = \mu E_R/M_0$, is 2.7 MPa, which is nine times greater than the global average

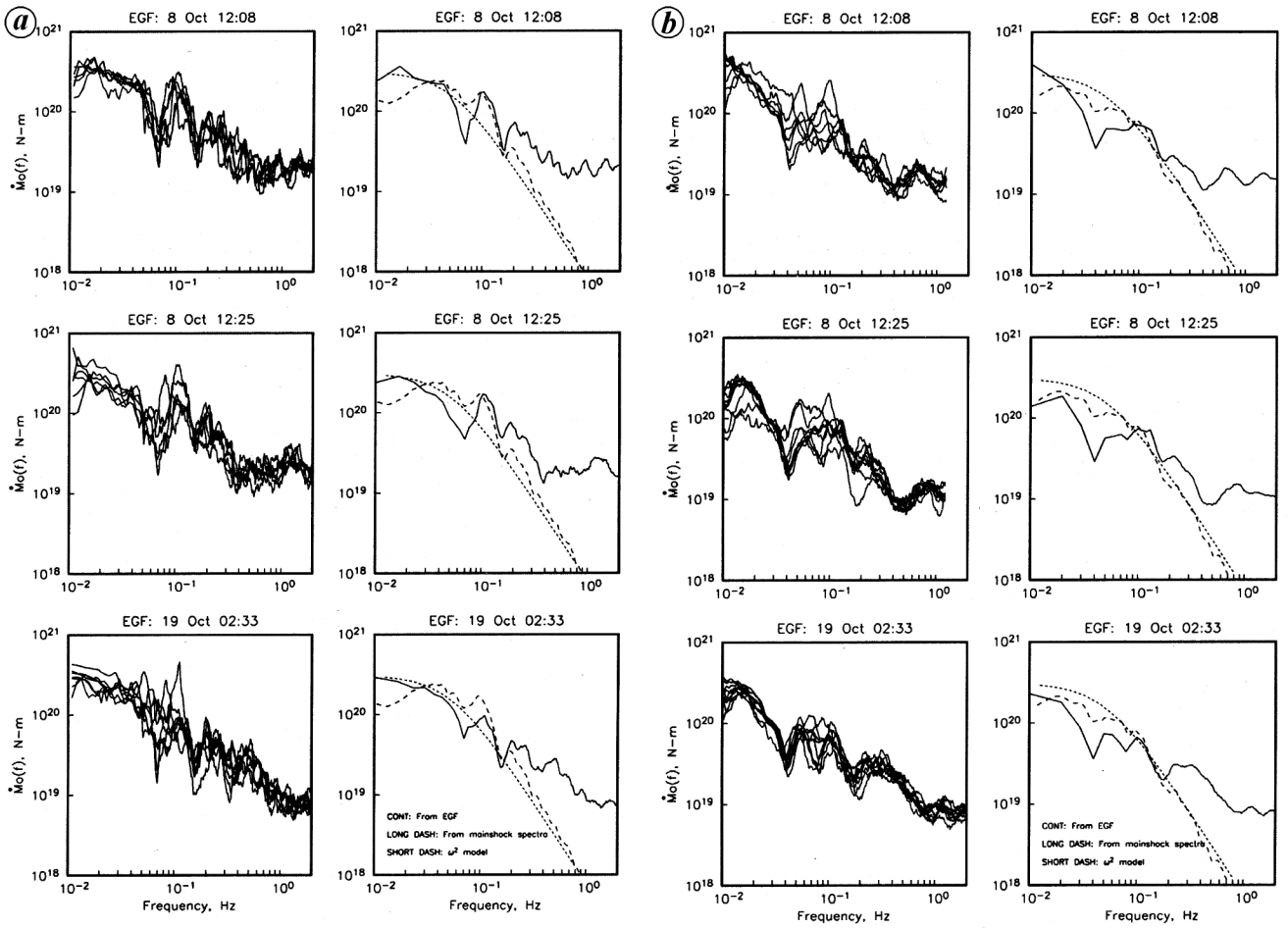

Figure 3. (Left frames) Moment rate spectra (MRFs) of Muzaffarabad mainshock estimated from spectral ratios of main shock to aftershocks (EGF technique) at individual stations. (Right frames) Median MRFs obtained by the EGF technique (continuous curves) and Lg-wave spectra (dashed curves). Superimposed on the right frames are dotted curves for an ω^{-2} source model ($M_0 = 2.94 \times 10^{20}$ N-m, $fc = 0.051$ Hz). (*a*) Data from IMD stations. (*b*) Data from non-IMD stations.

value reported for interplate thrust events at subduction zones[14].

The area of significant slip, mapped by Yagi[2], has a length L of ~100 km and width W of ~15 km. The static stress drop, $\Delta\sigma_s$, can be obtained from $\Delta\sigma_s = (8\mu/3\pi)(D/W)$, a relation[15] suitable for a shallow dip-slip fault with $L >> W$. Here D is the average slip which is given by the relation $M_0 = \mu LWD$. These relations yield $D = 6.7$ m and $\Delta\sigma_s = 11.3$ MPa for the Muzaffarabad event. We can now compute the radiation efficiency, η_R, which is defined as $\eta_R = E_R/(E_R + E_G) = (2E_R/M_0)/(\Delta\sigma_s/\mu)$, where E_G is the fracture energy[11]. The radiation efficiency of the Muzaffarabad event was ~0.49, similar to those of other large interplate earthquakes[11].

It is instructive to compare the Muzaffarabad earthquake with the Bhuj earthquake of 2001 (Table 2). Both events had the same moment magnitude, $Mw = 7.6$. The Bhuj earthquake was deeper than the Muzaffarabad earthquake. It radiated about the same energy as the latter event and its static stress drop was about two times larger. Radiation efficiency of the Muzaffarabad earthquake was twice that of the Bhuj earthquake. The energy magnitude, *Me*, of Muzaffarabad earthquake was about the same as that of the Bhuj earthquake. Thus, within the uncertainties involved in the estimation of such basic source parameters as E_R and $\Delta\sigma_s$, the two earthquakes are similar.

We have considered above, E_R estimated in this study from the regional data and the EGF technique to be accurate. If we assume that the radiated energy reported by Choy is correct, then the apparent stress becomes 0.37 MPa, which is close to the global average for interplate earthquakes at subduction zones[14]. However, in this case the radiation efficiency becomes very small, 0.06, suggesting an exceptionally large dissipation of energy in the fracture process of an interplate event.

Because of the similarity of source spectra of the earthquakes of Muzaffarabad and Bhuj, we expect similar ground motions from the two events. Figure 5 shows observed peak ground motions during the two earthquakes. A_{max} and V_{max} values for the Muzaffarabad earthquake are

Table 2. Comparison of source characteristics of Bhuj and Muzaffarabad earthquakes

Earthquake	$M_0 \times 10^{20}$ (N-m)	Mw	Depth range (km)	LXW (km^2)	$\Delta\sigma_s$ (MPa)	$E_R \times 10^{16}$ (J)	Me*	E_R/M_0	Radiation efficiency (η_R)
Bhuj[#] 26 Jan. 2001	3.40	7.6	10–35	1300	20	2.1	7.98	6.2×10^{-5}	0.23
Muzaffarabad 8 Oct. 2005	2.94	7.6	0–10	100 × 15**	11.3	0.29[+]	7.39	1.0×10^{-5}	0.06
						1.10[++]	7.79	3.7×10^{-5}	0.20
						2.70[+++]	8.05	9.1×10^{-5}	0.49

[#]Source parameters of Bhuj earthquake taken from Singh *et al.*[7].
*Computed from $Me = 2/3\log E_R - 2.9$, E_R in N-m (Choy and Boatwright[14]).
**Estimated from slip model of Yagi[2].
[+]E_R from G. Choy (written communication, 2006).
[++]E_R from H. Kanamori (written communication, 2006).
[+++]E_R estimated in this study using EGF technique.

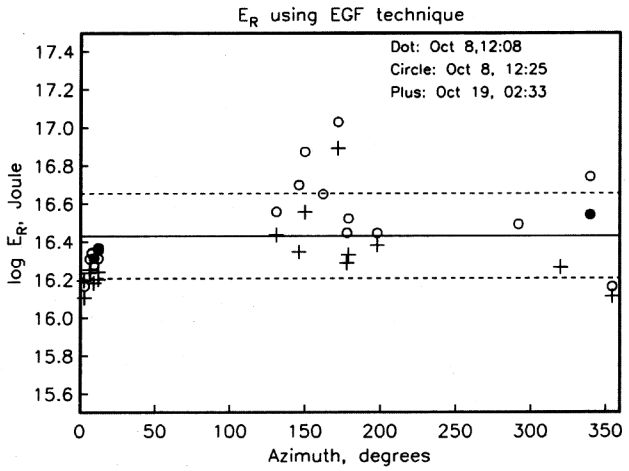

Figure 4. Radiated seismic energy, E_R, from the Muzaffarabad event estimated using three aftershocks as empirical Green's functions plotted as a function of azimuth. Continuous and dashed lines indicate median E_R and its ± one standard deviation.

slightly smaller (especially at the northern stations marked by triangles in Figure 5) than those recorded during the Bhuj event at similar distances. This may be attributed to the lower average Q for paths from the Muzaffarabad earthquake.

We followed the analysis of the Bhuj earthquake to infer near-source ground motions from the recordings in the far field using the stochastic method[6]. To accomplish this, we used an approximate finite-source model in which the fault area (assumed to be circular) is divided into small elements that rupture randomly with uniform probability over the source duration[16]. In this model the expressions for the Fourier spectrum of ground motion at distances much greater than the source dimension reduce to that of the ω^2-source model. Basic parameters assumed in the simulations were the same as those used above in the study of the source spectrum. Other parameters needed in the calculations were taken from the previous study of the Bhuj earthquake[6]. The Brune stress drop, $\Delta\sigma_B$, was taken as 10 MPa. Predicted A_{max} and V_{max} curves as a function of the closest distance to the fault, R, are shown in Figure 5. The curve for $Q = 800f^{0.42}$ fits the Bhuj data well, while curves for $Q = 500f^{0.62}$ and $300f^{0.62}$ explain the Muzaffarabad data recorded at stations to the south and north of the source respectively. Thus, the observed ground motions during both events are reasonably well explained by $\Delta\sigma_B \sim 10$ MPa, an anticipated result from the similarity of the source spectra. The intrapolation of the curves predict $A_{max} > 1$ g and $V_{max} > 100$ cm/s at $R = 1$ km. Our predicted peak ground motion at $R = 1$ km seems to be in agreement with seismic intensities of X reported in a preliminary geoseismological study of the earthquake by the Geological Survey of India[17]. We note that although the stress drops during the Bhuj and Muzaffarabad earthquakes were about the same, the ground motions in the epicentral area of the latter event may have been more intense than those during the former event because of its shallower source (hence smaller minimum R) and possible amplification of seismic waves due to rugged topography of the region.

The predictions from the stochastic method, however, underestimate the recorded peak ground motions during the 2006 event at the two closest stations, JMU and THN, by a factor of about two (Figure 5). It is possible to fit these datapoints by taking $\Delta\sigma_B = 20$ MPa. This would result in slight overestimation of the data recorded at longer distances. It would also predict A_{max} and V_{max} of about 3.5 g and 250 cm/s at $R = 1$ km. Relatively large values of A_{max} and V_{max} at JMU and TIEN may also be explained by other causes (such as site effect, directivity, etc.). We conclude that $\Delta\sigma_B \sim 10$ MPa explains reasonably well most, though not all, of the observed data.

The Muzaffarabad earthquake appears to be a typical interplate subduction earthquake if we consider its radiation efficiency. The source spectrum is close to a ω^2 model with a Brune stress drop of about 10 MPa. The normalized radiated energy, E_R/M_0 (and hence the apparent stress), and the static stress drop are relatively high. These source parameters are similar to those estimated for the Bhuj

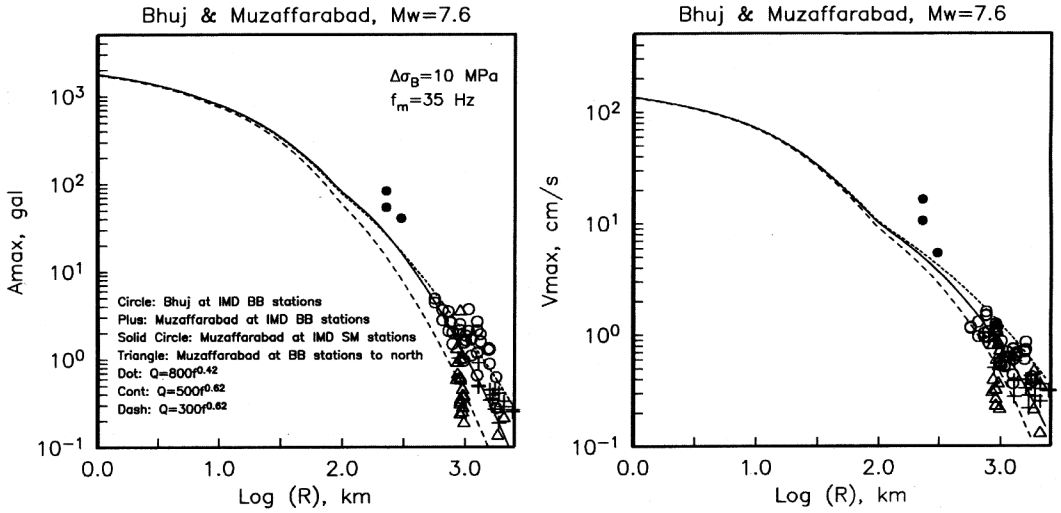

Figure 5. Horizontal component of A_{max} and V_{max} as a function of distance during the Muzaffarabad and Bhuj earthquakes. Plus, triangle, and solid circle: Muzaffarabad earthquake recorded at IMD BB station, non-IMD BB station, and IMD strong-motion station respectively. Circle: Bhuj earthquake recorded at IMD station. Predicted ground motions from an approximate finite-source model as a function of closest distance, R, from the fault are shown by curves. In these simulations, $\Delta\sigma_B = 10$ MPa. Curves corresponding to $Q(f) = 880f^{0.42}$ (dotted), $508f^{0.48}$ (continuous), and $300f^{0.48}$ (dashed) fit observed data from Bhuj and Muzaffarabad earthquakes recorded at IMD and non-IMD stations respectively.

earthquake that occurred in the 'stable' continental region. Peak ground motions predicted by the stochastic method with a stress drop of ~10 MPa fit reasonably well with the observed ones. It also predicts $A_{max} > 1$ g and $V_{max} >$ 100 cm/s above the epicentral zone. Here again, the Muzaffarabad earthquake is similar to the Bhuj event. These near-source ground motions, although in agreement with the field observations, must be considered a first rough guess. The complexity of the source process, rupture reaching the surface, and the rugged topography of the region must have given rise to a complex distribution of high peak values. Furthermore, physical models suggest asymmetry in the near-source ground motions with higher values on the hanging wall and relatively low values on the foot wall[18,19]. Near-field ground motion recordings during large/great earthquakes along the Himalayan arc are essentially non existent. Thus, the current effort in progress to install strong-motion stations in this region is most commendable.

1. http://www.seismology.harvard.edu
2. Inversion by Y. Yagi available at http://www.geo.tsukuba.ac.jp/press_HP/yagi/EQ/2005Pakistan/
3. Inversion by Chen Ji available at http://earthquake.usgs.gov/eqinthenews/2005/usdyae/finitefault/

4. Avouac, J., Ayoub, F., Leprince, S., Konca, O. and Helmberger, D., *Seismol. Res. Lett.*, 2006, **77**, 206.
5. Fielding, E., Pathier, E. and Wright, T., *Seismol. Res. Lett.*, 2006, **77**, 206.
6. Singh, S. K. *et al.*, *Bull. Seismol. Soc. Am.*, 2003, **93**, 353–370.
7. Singh, S. K., Pacheco, J. F., Bansal, B. K., Perez-Campos, X., Dattatrayam, R. S. and Suresh, G., *Bull. Seismol. Soc. Am.*, 2004, **94**, 1195–1206.
8. Singh, S. K., Ordaz, M., Dattatrayam, R. S. and Gupta, H. K., *Bull. Seismol. Soc. Am.*, 1999, **89**, 1620–1630.
9. Singh, S. K., García, D., Pacheco, J. F., Valenzuela, R., Bansal, B. K. and Dattatrayam, R. S., *Bull. Seismol. Soc. Am.*, 2004, **94**, 1564–1570.
10. Brune, J. N., *J. Geophys. Res.*, 1970, **75**, 4997–5009.
11. Venkataraman, A. and Kanamori, H., *J. Geophys. Res.*, 2004, **109**, B05302.
12. Vassiliou, M. S. and Kanamori, H., *Bull. Seismol. Soc. Am.*, 1982, **72**, 371–387.
13. Venkataraman, A., Rivera, L. and Kanamori, H., *Bull. Seismol. Soc. Am.*, 2002, **92**, 1256–1265.
14. Choy, G. and Boatwright, J., *J. Geophys. Res.*, 1995, **100**, 18,205–18,228.
15. Starr, A. T., *Proc. Cambridge Philos. Soc.*, 1928, **24**, 489–500.
16. Singh, S. K. *et al.*, *Bull. Seism. Soc. Am.*, 1989, **79**, 1697–1717.
17. http://www.gsi.gov.in/pokeq/kasheq.pdf
18. Brune, J. N., *Proc. Indian Acad. Sci. (Earth Planet. Sci.)*, 1996, **105**, L197–L206.
19. Brune, J. N. and Anooshehpoor, A., *Bull. Seismol. Soc. Am.*, 1998, **88**, 1070–1078.

ACKNOWLEDGEMENTS. We thank Hiroo Kanamori and George Choy for sharing their preliminary estimates of radiated energy, and Harsh Gupta for careful revision of the manuscript. We are grateful to the Director General, India Meteorological Department, New Delhi for permission to use the data. The research was partly funded by UNAM, DGAPA project IN114305 and CONACyT (Mexico) grant 42671-F.

Received 24 December 2005; revised accepted 4 May 2006